Available online at www.sciencedirect.com

ScienceDirect

Acta Materialia 85 (2015) 180–190

Acta MATERIALIA

www.elsevier.com/locate/actamat

Microstructurally based cross-slip mechanisms and their effects on dislocation microstructure evolution in fcc crystals

Ahmed M. Hussein,[a,*] Satish I. Rao,[b,c] Michael D. Uchic,[d] Dennis M. Dimiduk[d] and Jaafar A. El-Awady[a]

[a] *Department of Mechanical Engineering, Whiting School of Engineering, Johns Hopkins University, Baltimore, MD 21218-2682, USA*
[b] *UES Inc., 4401 Dayton-Xenia Road, Dayton, OH 45432-1894, USA*
[c] *Institute of Mechanical Engineering, EPFL, Lausanne, Switzerland*
[d] *Air Force Research Laboratory, Materials and Manufacturing Directorate, Wright-Patterson AFB, OH 45433-7817, USA*

Received 22 August 2014; revised 20 October 2014; accepted 30 October 2014

Abstract—Three newly identified cross-slip mechanisms from atomistic simulations of fcc crystals, namely surface, bulk and intersection cross-slip types, were hierarchically informed into discrete dislocation dynamics simulations. The influence of each cross-slip type on the evolution of the dislocation microstructure in face-centered cubic microcrystals having different crystal sizes and initial dislocation densities was investigated. Dislocation pattern formation, surface slip localization and initial strain hardening were observed, in agreement with experimental observations, and possible explanations are given in the light of these simulations.

Keywords: Cross-slip; Dislocation dynamics; Dislocation patterning; Strain hardening

1. Introduction

Dislocations are one of the most important microstructural features governing the mechanical properties of crystalline materials. They are the main carriers of plasticity, hence most of the related phenomena (e.g. yielding, strain hardening, strain-rate dependence, temperature dependence, etc.) depend on how the dislocation microstructure evolves and how dislocations interact with other material defects [1]. The dislocation microstructure evolution is an immensely complicated phenomenon that is controlled by material properties, microstructure and boundary conditions. Several mechanisms, such as dislocation dissociation, recombination, glide, cross-slip and climb, are active during material deformation and they all contribute to the final evolved microstructure [2]. Cross-slip of screw dislocations is recognized as one of the main mechanisms controlling dislocation multiplication in crystals [3,4], strain hardening [2,5–8], stress recovery during stage-III loading [9,10] and dislocation pattern formation [11]. Cross-slip also provides an effective mechanism for dislocations to bypass obstacles [12,13].

In attempts to describe the atomic scale mechanisms associated with cross-slip in face-centered cubic (fcc) crystals, several models have been proposed (e.g. [14–17]). For a critical review of these models, the reader is referred to the article by Puschl [18]. A number of experimental [19–22] and atomistic [23–26] studies have also been conducted over the years in order to identify the atomic mechanisms and estimate the activation parameters that are involved in the process. Nevertheless, to date, there is no universal agreement on how cross-slip takes place, and direct quantitative predictions of the influence of cross-slip on the mechanical properties are still subject to intensive studies. One reason why this problem is not very well understood is that the cross-slip phenomenon spans several length scales, starting at the atomic scale and going all the way up to hundreds of nanometers. However, the majority of previous studies of this phenomenon have focused on the atomistic length scale, hence a method for bridging these findings and making connections to larger length and time scales is still necessary.

One such model that could bridge this gap is discrete dislocation dynamics (DDD) simulations, in which both the time- and length-scale limitations from atomic simulations are greatly reduced. Over the past two decades, two-dimensional (2D) and three-dimensional (3D) DDD methods have been developed to simulate plastic deformation at the mesoscale in crystalline structures by direct numerical simulations of the collective motion of dislocation ensembles according to physics-based rules [27–34]. The physics that can be incorporated in DDD simulations can range

* Corresponding author; e-mail addresses: ahussei4@jhu.edu; jelawady@jhu.edu

http://dx.doi.org/10.1016/j.actamat.2014.10.067
1359-6462/

Report Documentation Page

Form Approved
OMB No. 0704-0188

1. REPORT DATE	2. REPORT TYPE	3. DATES COVERED
2015		**00-00-2015 to 00-00-2015**

4. TITLE AND SUBTITLE	5a. CONTRACT NUMBER
Microstructurally Based Cross-slip Mechanisms and Their Effects on Dislocation Microstructure Evolution in fcc Crystals	5b. GRANT NUMBER
	5c. PROGRAM ELEMENT NUMBER
6. AUTHOR(S)	5d. PROJECT NUMBER
	5e. TASK NUMBER
	5f. WORK UNIT NUMBER
7. PERFORMING ORGANIZATION NAME(S) AND ADDRESS(ES) **Johns Hopkins University,Department of Mechanical Engineering,3600 North Charles Street,Baltimore,MD,21218**	8. PERFORMING ORGANIZATION REPORT NUMBER
9. SPONSORING/MONITORING AGENCY NAME(S) AND ADDRESS(ES)	10. SPONSOR/MONITOR'S ACRONYM(S)
	11. SPONSOR/MONITOR'S REPORT NUMBER(S)

12. DISTRIBUTION/AVAILABILITY STATEMENT
Approved for public release; distribution unlimited

13. SUPPLEMENTARY NOTES

14. ABSTRACT

Three newly identified cross-slip mechanisms from atomistic simulations of fcc crystals, namely surface, bulk and intersection cross-slip types, were hierarchically informed into discrete dislocation dynamics simulations. The influence of each cross-slip type on the evolution of the dislocation microstructure in face-centered cubic microcrystals having different crystal sizes and initial dislocation densities was investigated. Dislocation pattern formation, surface slip localization and initial strain hardening were observed, in agreement with experimental observations, and possible explanations are given in the light of these simulations.

15. SUBJECT TERMS

16. SECURITY CLASSIFICATION OF:			17. LIMITATION OF ABSTRACT	18. NUMBER OF PAGES	19a. NAME OF RESPONSIBLE PERSON
a. REPORT	b. ABSTRACT	c. THIS PAGE			
unclassified	**unclassified**	**unclassified**	**Same as Report (SAR)**	**11**	

anywhere from the motion of simple infinite length (two-dimensional) dislocations in single crystals with periodic boundary conditions [35,36] to the complex dynamics and interactions of three-dimensional curved dislocations in single crystals or polycrystalline finite-sized materials [37]. DDD simulations were performed to study an array of material phenomena, including the response of thin films [38,39], size effects [40–43], irradiation hardening [44] and nanoindentation [45]. In addition, dislocation climb [46] and dislocation inertia effects at high strain rates [47] are among the physical behaviors that have been successfully implemented into DDD.

Cross-slip of screw-character dislocation segments in fcc crystals away from intersecting segments and forest dislocations (bulk cross-slip) was first introduced into 3D-DDD simulations by Kubin et al. [27] through a probabilistic procedure. In this approach, the cross-slip probability per time step, P_{step}, for any screw segment of length L, experiencing a local resolved shear stress on its glide plane and opposite to the applied shear stress, τ^g, is given by

$$P_{step} = \beta \frac{L}{L_o} \delta t \exp\left(\frac{(\tau^g - \tau_{III})V}{k_B T}\right) \quad (1)$$

where β is a scaling factor, L_o is a reference length of 1 μm, as defined in Ref. [27], δt is the time step, τ_{III} is the resolved shear stress at the onset of stage-III hardening for bulk crystals (i.e. parabolic hardening), V is the activation volume, k_B is the Boltzmann constant and T is the temperature. This equation was derived in accordance with the Escaig cross-slip model, which is based on a "phantom" obstacle resisting the motion of the dislocation and subsequently resulting in a constriction on the dislocation, leading to cross-slip [12]. This model has been the basis for incorporating cross-slip in most subsequent DDD simulation methods (e.g. [28,32,34,48]). It is worth noting that a similar form was used by Déprés et al. (2006); however, the resolved shear stress on the cross-slip plane was used rather than that on the glide plane [49]. A primary challenge to simulation studies using this model is that significant stresses are needed to activate the process, while generally there are no obstacles present within the idealized single crystal simulation cells to induce such stresses.

Recent molecular dynamics simulations have suggested that the activation energy of cross-slip should not be affected by the resolved shear stress on the glide plane; rather, the Escaig stress on both the glide and cross-slip planes have the dominant effect [50]. In addition, besides bulk cross-slip, a sub-group of the current authors have identified two new cross-slip mechanisms through molecular static and molecular dynamics simulations [51–55]. In the first such mechanism, intersection cross-slip, it was shown that cross-slip is preferentially observed at selected screw dislocation intersections in fcc crystals [51]. The activation energy was computed for cross-slip at attractive forest dislocation intersections and was shown to be 2–5 times lower than that for bulk cross-slip [52,53]. Furthermore, spontaneous (i.e. athermal) cross-slip was also observed to occur at mildly repulsive intersections [54]. In the second mechanism, surface cross-slip, it was reported that a negative constriction forms on screw dislocations ending at free surfaces under certain conditions and that the activation energy for cross-slip is significantly lower than that for cross-slip at attractive forest dislocation intersections [55]. These new rules promote the need to revise how cross-slip is incorporated into DDD simulations.

Accordingly, the motivation of the current work is to incorporate an atomistically informed cross-slip model into DDD simulations of fcc crystals. The details of the computational model are presented in Section 2. Simulation results of the deformation of single-crystal nickel microcrystals of various sizes and at different dislocation densities using this model are presented in Section 3. Further insights into the effect of cross-slip on dislocation evolution, microstructure patterning and slip band thickening are discussed in Section 4. Finally, a summary and conclusions are presented in Section 5.

2. Computational method

All simulations performed in this study employ the 3D-DDD open source code, ParaDiS, originally developed at Lawrence Livermore National Laboratory [33]. In ParaDis, the dislocations are discretized into short linear segments that can be arbitrarily interconnected. The open source code was modified in-house to guarantee that, for simulations of fcc crystals, dislocation collisions and glide will always remain co-planner on the correct slip systems. The code was also extended as described below to incorporate the mechanisms of bulk, surface, attractive intersection and repulsive intersection cross-slip, as identified from atomistic simulations.

In order to effectively handle the most general cases of cross-slip, a search algorithm that employs graph-theoretic approaches was used in order to detect the longest possible screw-character dislocation chains, which are sequences of dislocation segments. Here, each dislocation segment is a straight line connecting two dislocation nodes. Identifying long chains reduces the number of cross-slip events handled computationally, rather than individually computing cross-slip probabilities for several parts of the same chain. More importantly, because the probability of cross-slip increases linearly with the length of the screw dislocation chain, handling shorter chains can cause some potential cross-slip events to pass undetected. Next, the appropriate cross-slip type is identified depending on the configuration of the dislocation chain in the crystal, according to the following rules. If a screw dislocation chain intersects a free surface, it is considered a surface cross-slip type candidate. If the chain fully resides inside the crystal and it intersects with another dislocation not lying on either its glide or cross-slip plane, then it is considered to be an intersection cross-slip type candidate. Further, if the sum of the two Burgers vectors of the intersecting dislocations is $\langle 1\,1\,2\rangle$, the screw dislocation chain is determined to be a repulsive intersection cross-slip type, which is a spontaneous process that does not require any activation energy to take place [54]. On the other hand, if the sum of the Burgers vectors is $\langle 1\,0\,0\rangle$ then it is considered to be a Hirth-lock attractive cross-slip type candidate. If the Burgers vectors sum is $\langle 1\,1\,0\rangle$ and the intersecting dislocations are on $\{1\,1\,0\}$ or $\{1\,0\,0\}$ planes, then it is considered as an attractive intersection Lomer–Cottrel (LC) cross-slip type candidate. If the vectors sum is $\langle 1\,1\,0\rangle$ and the intersecting dislocations are on $\{1\,1\,1\}$ slip planes, then it is considered as an attractive intersection glide-lock cross-slip type candidate. Finally, if the screw dislocation chain does not satisfy any of the above condi-

tions, it is considered as a bulk cross-slip type candidate. A flowchart describing these proposed rules as incorporated into the DDD framework is shown in Fig. 1. In the current simulations, dislocation chains are considered to be of a screw character if they lie within an angle of 15° from the Burgers vector direction.

After identifying the potential cross-slip type, all screw dislocation chains are subjected to two additional rules to check whether cross-slip is favorable for this chain or not. First, the magnitude of the resolved shear stress on the cross-slip plane should be greater than or equal to the magnitude of the resolved shear stress on the glide plane. Second, the resolved shear stress on the cross-slip plane must be equal to or greater than $\frac{\mu b}{10L}$, where μ is the shear modulus, b is the Burgers vector magnitude and L is the screw dislocation length. These two rules guarantee that the dislocation will glide away after it cross-slips. Since, except for repulsive intersection type cross-slip events, which are athermal, cross-slip is a thermally activated mechanism, the frequency of cross-slip events during the simulated time step can be computed through an Arrhenius-like equation similar to that developed by Kubin et al. (1992), such that:

$$f = \omega_a \frac{L}{L_o} exp\left(-\frac{(E_a - V_a \Delta\tau_E)}{k_B T}\right) \tag{2}$$

Here, E_a is the energy barrier required to form a constriction point on the screw dislocation, which depends on the type of cross-slip under consideration. $\Delta\tau_E = \tau_E^g - \tau_E^{cs}$ is the difference between the Escaig stress on the glide plane and that on the cross-slip plane, as recent MD simulations have shown that the energy barrier for cross-slip decreases with increasing Escaig stress on the glide plane, τ_E^g, and decreases with increasing Escaig stress on the cross-slip plane, τ_E^{cs} [50]. The Escaig stress is the stress component resolved onto the slip plane along a direction that brings the two Shockley partial dislocations closer together or pushes them farther away from each other, depending on its sign. In addition to the stacking fault energy and the interaction stresses between the dislocation partials, the Escaig stress is the component of the applied stress that controls the stacking fault width. It can be obtained by constructing a local coordinate system where the Z-axis is the slip plane normal, the X-axis is in the direction of the Burgers vector and the Y-axis is mutually perpendicular to both the X- and Z-axes according to the right-hand screw rule. By transforming the stress tensor to this new coordinate system, the Escaig stress would be the σ_{yz} component of the stress tensor. Since the dislocation is of a screw character, line directions of the perfect dislocations and its partials are all parallel to the X-axis of the local coordinate system. The Escaig stress acts on the edge components of the partial dislocations (which are in opposite directions so that they cancel out) and causes them to either combine (for a positive Escaig stress) or further repel (for a negative Escaig stress). In addition, V_a is the activation volume defining the rate by which the Escaig stress decreases the cross-slip energy barrier (note the difference between the cross-slip energy barrier, $E_a - V_a\Delta\tau_E$, and the constriction formation energy barrier, E_a). The cross-slip frequency is

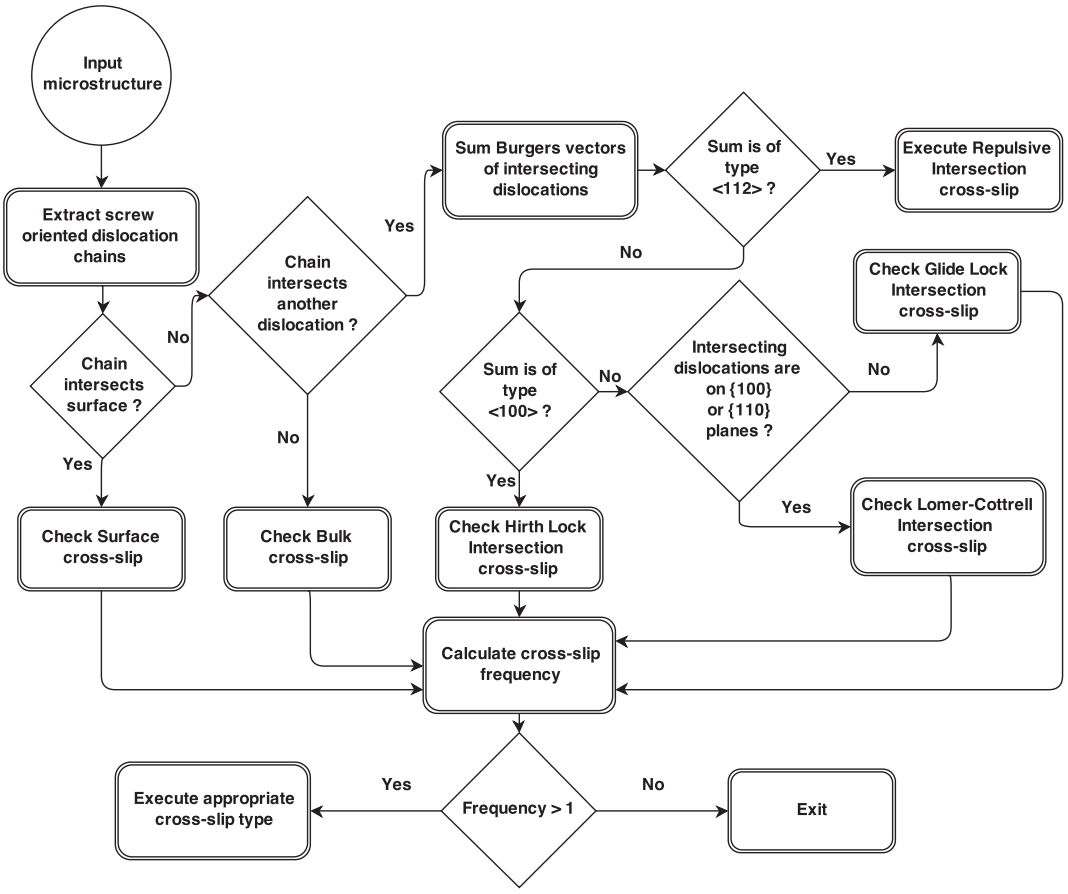

Fig. 1. Flowchart of the proposed rules for cross-slip mechanisms as incorporated into the DDD framework.

computed based on an attempt frequency $\omega_a = \eta\omega_D$, where ω_D is the Debye frequency of the material and the scaling factor η, which is the ratio of the simulation strain rate to the experimental strain rate, is used in order to get the same number of cross-slip attempts in the same time interval. The reference length L_o is the screw dislocation chain length at which bulk cross-slip occurs with a probability of 1 in a 1 s time interval at room temperature for conditions where the Escaig stresses on the glide and on the cross-slip planes are identical, and where the cross-slip attempt frequency is equal to the Debye frequency. Since the number of constrictions scales linearly with the length of the screw dislocation L, the expression is scaled by L/L_o.

Finally, if the frequency defined by Eq. (2) is greater than one, then cross-slip should occur. For intersection and bulk cross-slip cases, the dislocation length L is a small arbitrary value that can be fitted to match the experimental results, while for bulk cross-slip, it is the actual length of the screw dislocation chain. This is because the constriction energies of surface and intersection cross-slip are lower for the portion of the dislocation near the surface or at the intersection point, while it is the same as the bulk constriction energy for the remaining length of the dislocation. In this work, the surface and intersection cross-slip lengths are chosen to be 1.25 and 2.5 nm, respectively.

The energy barrier and activation volume in Eq. (2) are determined based on the cross-slip type under consideration. In the current simulations, these values were computed from atomistic simulations for nickel [51–55], and are summarized in Table 1. In order to emulate experiments and get a similar number of cross-slip events, the Debye frequency, which is on the order of (10^{13} s^{-1}), was scaled by the ratio of the experimental strain rate, 10^{-3} s^{-1}, to the simulation strain rate, 50 s^{-1}, which gives an attempt frequency of $\omega_a = 5 \times 10^{17}$ s^{-1}. To significantly improve the numerical efficiency of the simulations, a minimum dislocation chain length of four dislocation segments was enforced in order to prevent the successive redundant oscillations of very short dislocation chains between the glide and cross-slip planes. If the chain is determined to be a repulsive cross-slip candidate, or if the above two rules are satisfied for all other cross-slip types, cross-slip is realized by changing the glide planes of the entire screw dislocation chain.

All simulation cells modeled hereafter have square cross-sections, with edge-length D. For simulation cells with $D \leqslant 5$ μm, a height-to-edge ratio of $L/D = 3$ was chosen, while the height-to-edge ratio for larger crystals was $L/D = 1$ due to computational difficulties. A uniformly increasing tensile stress was imposed on the crystal such that a nominal strain rate control of 50 s^{-1} is maintained. All simulation cells are oriented for multislip deformation in the [0 0 1] direction. The material properties of nickel single crystals were chosen, and the initial dislocation density was varied between 5×10^{10} m^{-2} and 10^{13} m^{-2}, while the simulation cell edge-length was varied between 0.5 μm and 10 μm.

The initial dislocation microstructure consisted of Frank–Read sources generated randomly on the {1 1 1} family of planes, with the overall line orientation making arbitrary angles with the Burgers vector directions. The lengths of the initial sources were normally distributed, with a mean that scales with the grain size and a standard deviation that is 10% of the mean length. It should be noted that it has been verified in the literature that introducing random pinning points (e.g. Frank–Read sources, as in our current study) gives quantitatively the same response in terms of size-scale effects as simulations starting from an initially pin-free dislocation network for the same relaxed dislocation densities [41].

Table 1. Nickel Cross-slip parameters.

Cross-slip type	Activation energy, E_a	Activation volume, V_a
Bulk	$0.8eV$	$20b^3$
Surface	$0.2eV$	$20b^3$
Hirth-lock	$0.2eV$	$20b^3$
LC lock	$0.6eV$	$20b^3$
Glide lock	$0.5eV$	$20b^3$

3. Simulations results

The effect of cross-slip on the engineering stress–strain response and the evolution of the dislocation density are shown in Fig. 2 for four representative crystal sizes of $D = 0.5$, 1.0, 5.0 and 10.0 μm. For each size, the results from simulations accounting for all cross-slip types and simulations without cross-slip are shown. For crystal sizes $D = 0.5$ and 1.0 μm, no clear effect of cross-slip on the flow stress is observed, as can be seen in Fig. 2(a). Both the simulations with and without cross-slip show no strain hardening up to 0.8% strain. In addition, the average dislocation density is weakly affected by cross-slip and remains relatively constant throughout the simulations, as shown in Fig. 2(b). Nevertheless, it is clear that more significant dislocation bursts are observed in simulations with cross-slip, as evident by the larger stress drops and accompanying dislocation density spikes.

On the other hand, significant early stage strain hardening can be observed for the $D = 5.0$ μm case and a lower hardening rate can be observed for the $D = 10.0$ μm case, as shown in Fig. 2(c). In addition, as shown in Fig. 2(d), the dislocation density increases rapidly for both crystal sizes in the presence of cross-slip. At 0.5% strain, the dislocation density in both crystal sizes is observed to increase by an order of magnitude from the initial dislocation density, while simulations without cross-slip show a steady-state dislocation density throughout the simulation.

Fig. 3 shows the number of junctions as a function of engineering strain from the simulations of the four crystal sizes reported in Fig. 2. Both simulations with all types of cross-slip and without any cross-slip are shown. Two observations can be made here. First, the number of junctions increases more significantly in the presence of cross-slip as compared to simulations without cross-slip. Second, the number of junctions increases more rapidly for the $D = 5.0$ and 10.0 μm crystals as compared to the two smaller crystals.

Fig. 4 shows the initial and final dislocation microstructures from simulations with and without cross-slip for the cases reported in Fig. 2. It is clear that, while the initial dislocation density in the smaller two samples is double that in the larger samples, no clear dislocation density build-up is observed in the smaller crystals either with or without cross-slip. Similarly, no clear dislocation build-up is observed for the two larger simulations without cross-slip, even though multiple sources were activated throughout

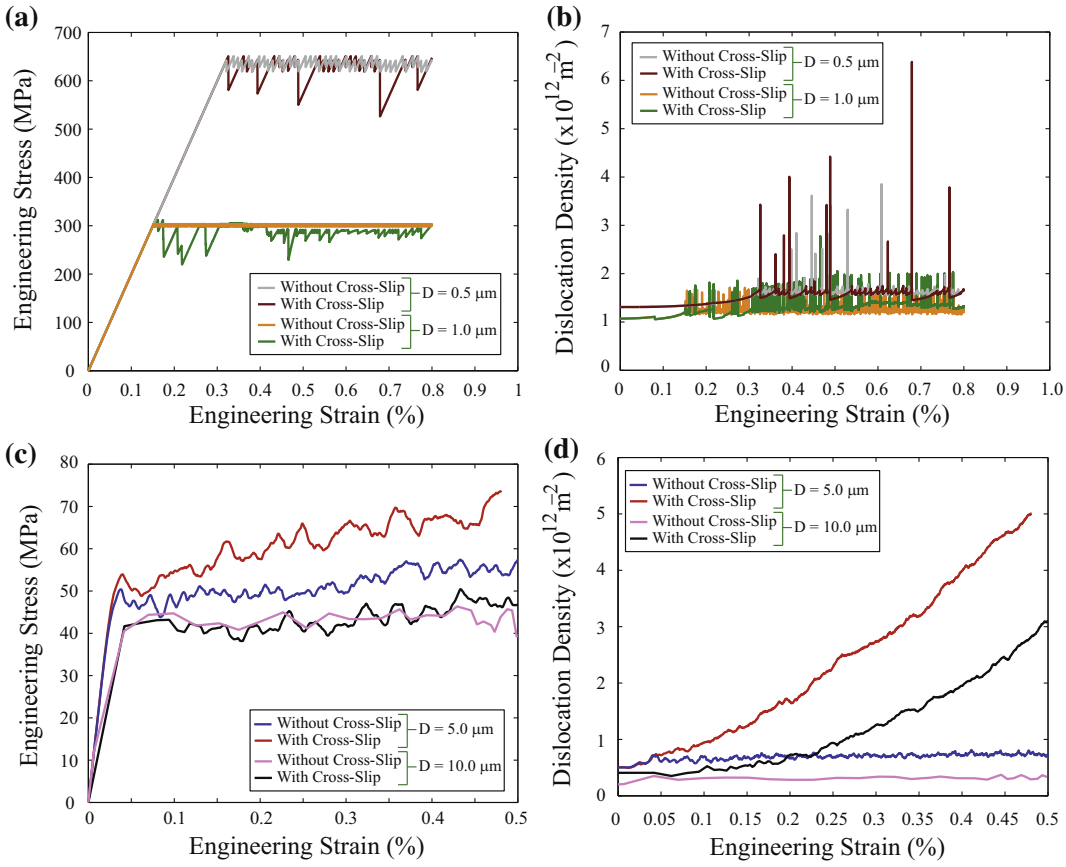

Fig. 2. (a, b) Engineering stress and dislocation density vs. engineering strain, respectively, for $D = 0.5$ and 1.0 μm simulation cells. (c, d) Engineering stress and dislocation density vs. engineering strain, respectively, for $D = 5.0$ and 10.0 μm simulation cells.

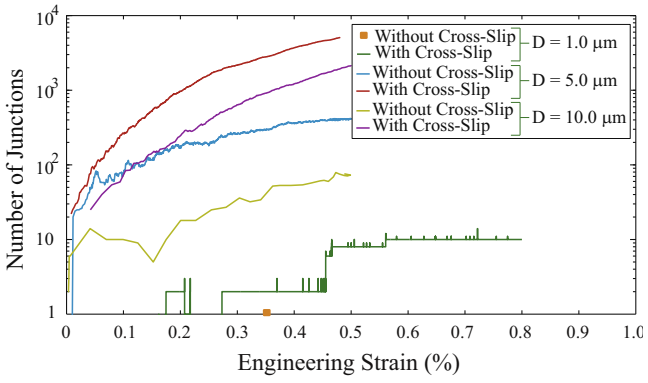

Fig. 3. Number of junctions vs. engineering strain for the $D = 1.0, 5.0$ and 10.0 μm microcrystals discussed in Fig. 2 with and without cross-slip. No junctions were found in the $D = 0.5$ μm microcrystal in simulations with or without cross-slip.

the simulations. On the other hand, in the same two larger samples, when all cross-slip types are accounted for, a dislocation build-up is clearly observed, showing an early stage self-organization in high dislocation density walls and lower dislocation density channels. The dislocation walls form mainly at the center of the crystal, creating partial dislocation cell structures that intersect the crystal surfaces. Animations of the 3D microstructures showing the dislocation pattern formation in the $D = 5.0$ and 10.0 μm crystals are shown in the supplementary movie1.avi and movie2.avi, respectively.

In order to investigate the effect of the different cross-slip types on the evolution of the dislocation microstructure, the simulations were repeated with the same initial dislocation network but with only one cross-slip mechanism enabled at a time. The initial dislocation density in these simulations was 5×10^{11} m^{-2} and the crystal size was $D = 5.0$ μm. Fig. 5 shows the predicted microstructures from these simulations at 0.25 % strain. Fig. 5(a) shows the predicted dislocation microstructure from simulations taking into account only bulk cross-slip, with all other cross-slip types being disabled. Similarly, the dislocation microstructure from simulations accounting only for intersection cross-slip and for surface cross-slip are shown in Fig. 5(b) and (c), respectively. It is clear from these results than no distinct dislocation pattern emerges from any of these simulation cases up to 0.25 % strain. On the other hand, when all cross-slip types are accounted for in the simulations, the microstructure shows a clear pattern formation, starting even at such a relatively low strain level, as shown in 5(d). It should be noted that it might be possible to develop dislocation patterns in simulations accounting only for one cross-slip type at much higher strains. However, with all cross-slip types accounted for, it is clear that the dislocation pattern is predicted to emerge at much lower strain levels. Recent experimental observations on fcc metals [56–58] have confirmed the emergence of dislocation patterns at strain levels close to the ones predicted by these simulations.

Cross-slip was also found to influence the formation of surface slip traces on the crystal surface. Fig. 6 shows the

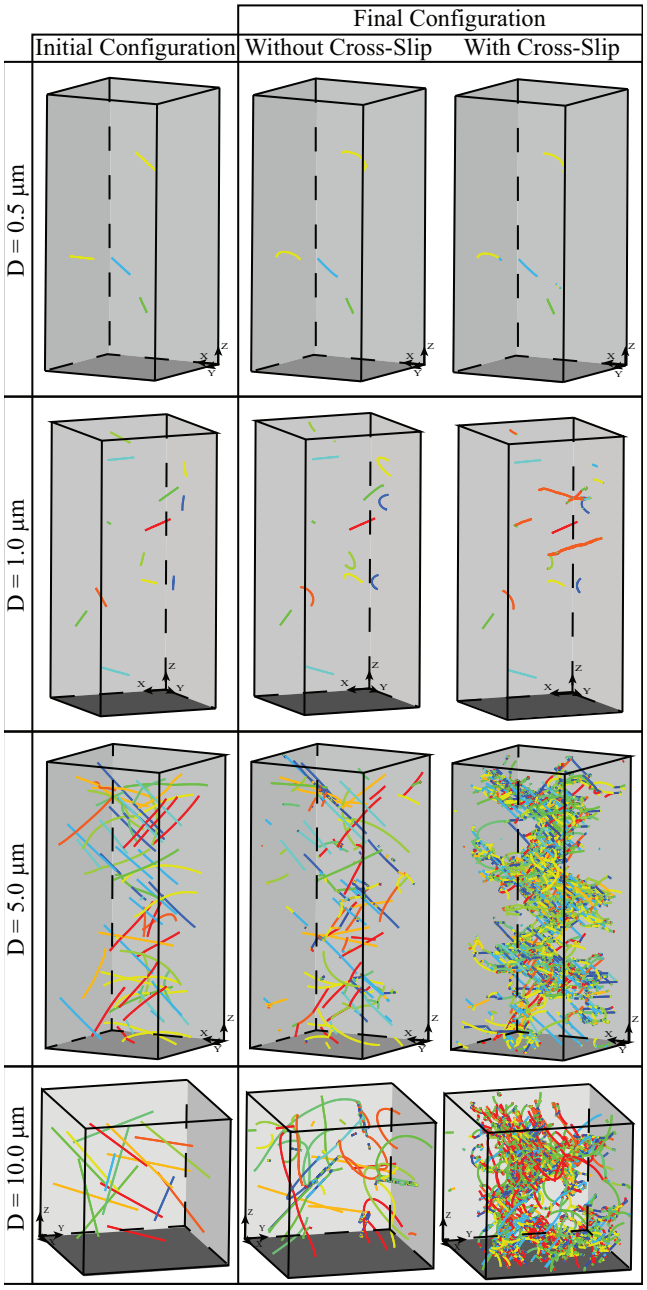

Fig. 4. The initial and final dislocation configurations in the four microcrystals discussed in Fig. 2 with and without cross-slip. The final configurations are reported at 1.0% strain for the $D = 0.5\ \mu$m and $D = 1.0\ \mu$m crystals, and at 0.5% strain for $D = 5.0\ \mu$m and $D = 10.0\ \mu$m crystals.

dislocation microstructure and the corresponding surface slip traces at different strain magnitudes from DDD simulations of a $D = 20.0\ \mu$m simulation cell initialized with a single Frank–Read source of length 8.0 μm, which corresponds to an initial dislocation density of $10^9\ \mathrm{m}^{-2}$. A strong shear localization is first observed on the slip plane of the original Frank–Read source. However, as plasticity evolves, multiple secondary localized slip bands are observed on two specific slip systems, one parallel to the original Frank–Read source plane and the other parallel to its cross-slip slip plane. The density of these slip bands and their heights increase with increasing strain. It is clear that the slip band thickening is accommodated by an increase in dislocation density in the crystal on multiple slip systems. It should be noted that the slip activity is not simultaneous but, rather, intermittent, with slip occurring on different planes for a limited time, then suppressed while slip commences on other planes. Slip band patterns similar to the one presented here have been experimentally observed in fcc single crystals [43,59]. Fig. 6(g) shows slip band patterns from an Ni microcrystal having a 20.0 μm diameter after 12.7 % strain [43] qualitatively showing similar patterns to the current simulations.

4. Discussion

4.1. Cross-slip effects on dislocation microstructure pattern formation

Dislocation pattern formation is a self-organizing phenomenon occurring at the grain length scale, which is typically in the micron and sub-micron ranges. The formation and evolution of dislocation patterns during the deformation of fcc single crystals has been well characterized experimentally in large crystals. Dislocation cell structures have been routinely observed in all stages of deformation, with the dislocation cell size decreasing with increasing strain [60]. Furthermore, in situ transmission electron microscopy tensile tests of pre-strained single crystals Al thin films also show the accumulation of dislocations within a cell boundary at stage-III of strain hardening in double slip conditions [61]. More recently, in situ scanning electron microscopy compression experiments of Al microcrystals oriented for multislip have shown that the formation of dislocation cells is observed when the crystal size is $D > 2.5\ \mu$m. However, no dislocation cells were observed in smaller crystals [62]. In the current DDD simulations, when accounting for all cross-slip types, dislocation microstructure pattern formation is clearly observed during the deformation of microcrystals having sizes $D = 5.0$ and 10.0 μm, as observed in Fig. 4. On the other hand, for microcrystals having sizes $D = 0.5$ and 1.0 μm, no dislocation patterns were evident. These results qualitatively agree with the experimental observations, and suggest that dislocation cell structures are suppressed due to the geometric limitations of the crystal when the crystal size is $D \leqslant 5.0\ \mu$m, with initial dislocation densities in the range of 5×10^{11} to 5×10^{12}. It should be noted that this critical size could be strongly dependent on the initial dislocation density since a bulk-like response can be expected for any crystal size if the dislocation density is above a critical value [63,65].

As was shown in Section 3, there is an increase in the number of junctions formed when cross-slip is active, and the number of junctions increases more rapidly for the larger $D = 5.0\ \mu$m and $D = 10.0\ \mu$m crystals. This is mainly due to the much shorter distance a dislocation can travel in the smaller crystals before exiting the crystal, thus reducing the probability of intersecting other dislocations, even with cross-slip fully accounted for. The dislocation pattern formation is observed to be associated with an enhanced dislocation junction formation. A junction in the current simulations is identified as any dislocation node where three or more dislocation segments, usually belonging to different slip systems, intersect. Junctions are typically difficult to move since they must satisfy glide restrictions of all intersecting dislocations slip systems simultaneously. If the

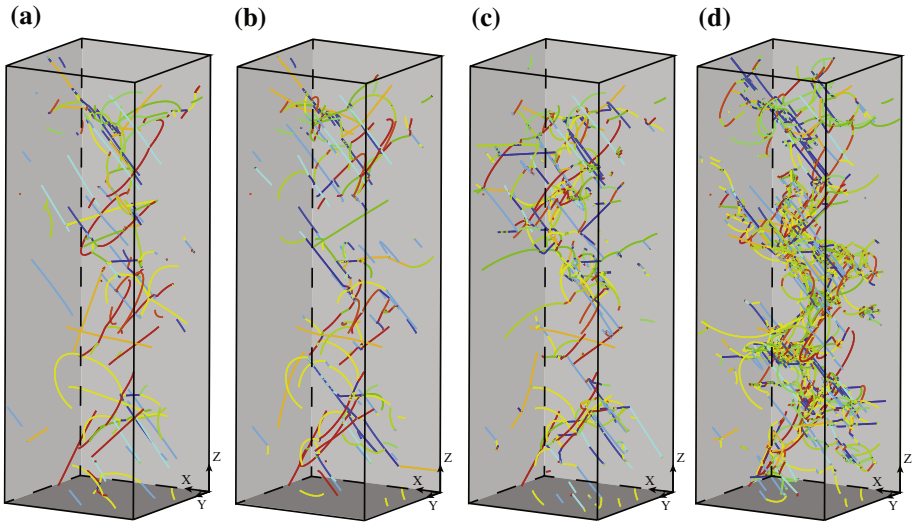

Fig. 5. Dislocation microstructure at 0.25 % strain for simulations starting with the same initial dislocation network while accounting for (a) only bulk cross-slip, (b) only intersection cross-slip, (c) only surface cross-slip and (d) all cross-slip types. The simulation cell had size $D = 5.0\ \mu$m and the initial dislocation density was $5 \times 10^{11}\ \mathrm{m}^{-2}$. Dislocations are colored based on the slip system.

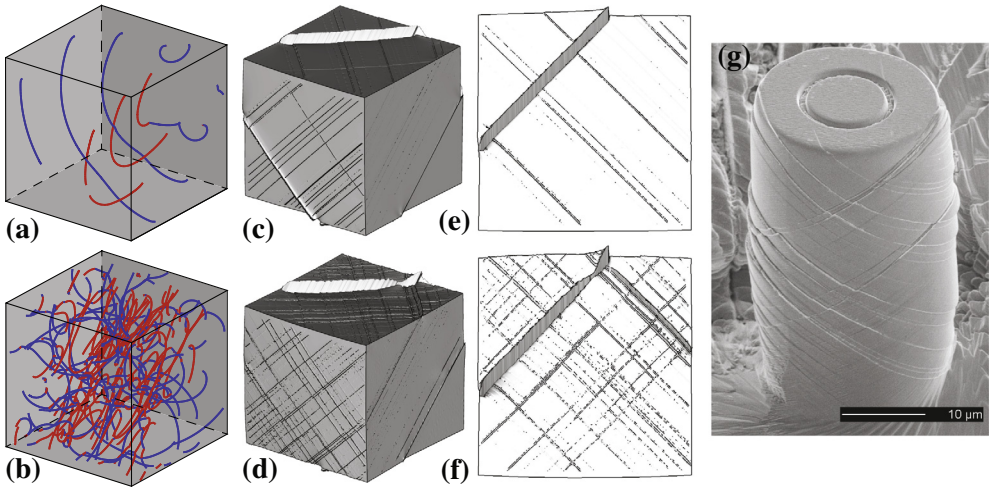

Fig. 6. Dislocation microstructure at (a) 0.15% and (b) 0.3% strain. The corresponding 3D surface slip traces are shown in (c) and (d), while a top view is shown in (e) and (f), respectively. The simulation cell is $D = 20.0\ \mu$m and a single Frank–Read source of length 8.0 μm was introduced in the cell, which corresponds to an initial dislocation density of $10^9\ \mathrm{m}^{-2}$. Dislocations are colored based on the slip system, and the initial dislocation corresponds to the blue slip system. (g) Slip band patterns from a 20.0 μ diameter Ni microcrystal after 12.7% strain qualitatively showing similar patterns to the current simulations [43].

intersecting dislocation segments lie on three or more different slip planes, then the junction will remain immobile. In our current simulations, in most cases, once the junction forms, it is difficult to break. Thus, junctions typically serve as sites at which high dislocation density build-up is observed, which subsequently promotes dislocation patterning.

Cross-slip, in general, helps redirect dislocations around obstacles that block their glide. These obstacles are forest dislocations in the current study. Cross-slip can also aid in propagating dislocations to glide on a different slip planes where the resolved shear stress is higher. As dislocations cross-slip, the probability of them interacting with other dislocations on other slip systems increases and subsequently the number of junctions increases. Thus, cross-slip acts as a mechanism by which the substructure evolves throughout the crystal. This is in contrast with the no cross-slip case, where the dislocations remain on their original planes without the potential of multiplying on other slip planes, thus limiting the number of junction sites. On the other hand, the crystal size plays an important role in the formation of dislocation patterns as well. If the crystal size is small, dislocations have a higher probability of escaping the crystal before interacting with other dislocations and forming strong junctions. This is evident in the $D = 0.5$ and 1.0 μm microcrystals, which show only a modest increase of junctions in the presence of cross-slip. As previously stated, an increasing dislocation density would lead to an increasing number of strong junctions in smaller crystals, which could subsequently lead to pattern formation in these crystals. However, the dislocation densities modeled here in the two smaller crystals are 1–2 orders of magnitude smaller than the typical dislocation density at which a bulk response is expected to be recovered [63].

Previously published DDD simulations accounting for only bulk cross-slip, as implemented using Eq. (1), have also suggested the formation of dislocation "cell-like" structures in large simulation cells ($\approx 10.0\ \mu m^3$) with periodic boundary conditions imposed [11]. However, in the presence of free surfaces, similar structures were only reported in much larger simulation cells ($15.0\ \mu m^3$) [65]. From the individual cross-slip type simulations, it is clear that the local dislocation density build-up in the crystal is not strong enough to form a well-defined pattern at the strain levels reached here. On the other hand, when all cross-slip mechanisms are accounted for, a much clearer dislocation structure is observed. Further analysis on the rate of new dislocation source generation from these individual cross-slip type simulations is discussed in Section 4.3.

4.2. Surface slip nand thickening

Formation of surface slip traces and steps is a natural consequence of dislocation interactions with crystal surfaces. It is generally common to observe these slip traces distributed randomly on the crystal surface in bulk [66,68] and microcrystals [68,70], with the slip trace density and step hight depending on the strain. Slip typically concentrates on a few planes with rather strong shear, in addition to the formation of localized slip bands along the length of the deforming crystal length. The formation of localized slip bands might be surprising, especially for microcrystals containing few initial dislocation sources (equivalently at dislocation densities on the order of $10^{12}\ m^{-2}$).

In the absence of cross-slip, DDD simulations typically show localized strong shear on a limited number of slip planes, with no clear slip band formation [34]. However, in our current simulations with cross-slip, localized slip bands are commonly observed in all simulated crystal sizes. In the following we examine surface cross-slip as a potential mechanism responsible for the formation of localized slip bands in microcrystals. Upon taking a closer look at the microstructure evolution, a specific repeating mechanism was observed to take place. When a bulk dislocation intersects a free surface, the dislocation splits into a surface step of height **b** and two single-ended dislocation segments that continue to glide away, extending the surface step. If either of the two single-ended dislocations reaches a screw orientation as it continues to glide, and given the low surface cross-slip activation energy, it can subsequently cross-slip on the surface and glide on a new glide plane. Similarly, after the dislocation cross-slips, it can further double cross-slip on the surface and start gliding on a third plane, which is parallel to its original plane. Because the surface cross-slip activation energy is relatively low, these dislocations can keep cross-slipping in this manner until an array of dislocations, all gliding on parallel planes, are created. All these dislocations have originated from the same initial source and subsequently their interaction with the free surface will result in a localized slip band. Fig. 7 shows the four steps of this process schematically.

At the beginning of the slip band formation, the dislocation traverse distance is almost purely stochastic and the second cross-slip event can occur anywhere. However, as the dislocation array gets denser, the stresses from the dislocations gliding on parallel planes can reduce the surface cross-slip activation energy further. Thus, the local stress field can become the influencing factor in cross-slip probability, and dislocations would preferentially cross-slip on unoccupied parallel planes where the back stresses are relatively lower, rather than a plane occupied by other dislocations on which the back stresses are relatively higher.

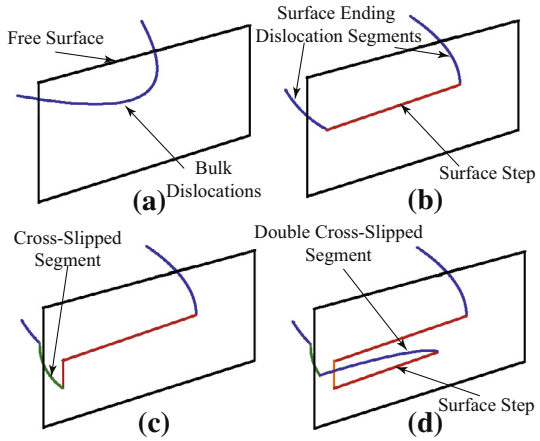

Fig. 7. A schematic showing the surface slip localization mechanism. The blue and green dislocations lie inside the crystal on slip planes P1 and P2, respectively, while the red surface segments represent dislocation segments that exited the crystal. In (a) a dislocation approaches the surface on P1. In (b) the dislocation intersects the surface forming a surface step represented by the red line. In (c) one of the surface intersecting dislocation segments cross-slips and glides onto P2, as shown by the green segment. This results in a new surface step on P2. In (d) the newly formed segment on P2 cross-slips back to a plane parallel to P1 and subsequently forms another surface step on that plane parallel to the first surface step on P1. The two blue dislocations in (d) glide on two parallel planes. (For interpretation of the references to colour in this figure legend, the reader is referred to the web version of this article.)

4.3. Cross-slip statistics

It is of interest to quantify the influence of each cross-slip type on the evolution of dislocations in the crystal. It is particularly important to identify the effect of each cross-slip type on the rate of generation of new dislocation sources in an effort towards developing dislocation density evolution continuum models [71]. Towards that goal, Fig. 8 shows the number of new sources formed, after 0.5 % strain, due to each cross-slip type as a function of initial dislocation density and crystal size from all the simulations. The crystal sizes were varied between $D = 0.5, 1.0, 5.0$ and $10.0\ \mu m$, and the initial dislocation density was varied between 5×10^{10} and $10^{13}\ m^{-2}$.

As seen in Fig. 8, there is a positive correlation between the source generation and the crystal size. Whereas bulk cross-slip source generation is not very sensitive to crystal size, surface and intersection cross-slip source generation show significant sensitivity. Smaller crystals, especially at low dislocation densities, do not show significant source generation by cross-slip compared to larger crystals in general. Furthermore, for a given initial dislocation density, the larger the crystal size the more dislocation sources it will contain and, consequently, the higher the number of sources being generated. A possible explanation for this is that, for larger crystals, the probability of dislocation collisions and subsequent junction formation is higher than that

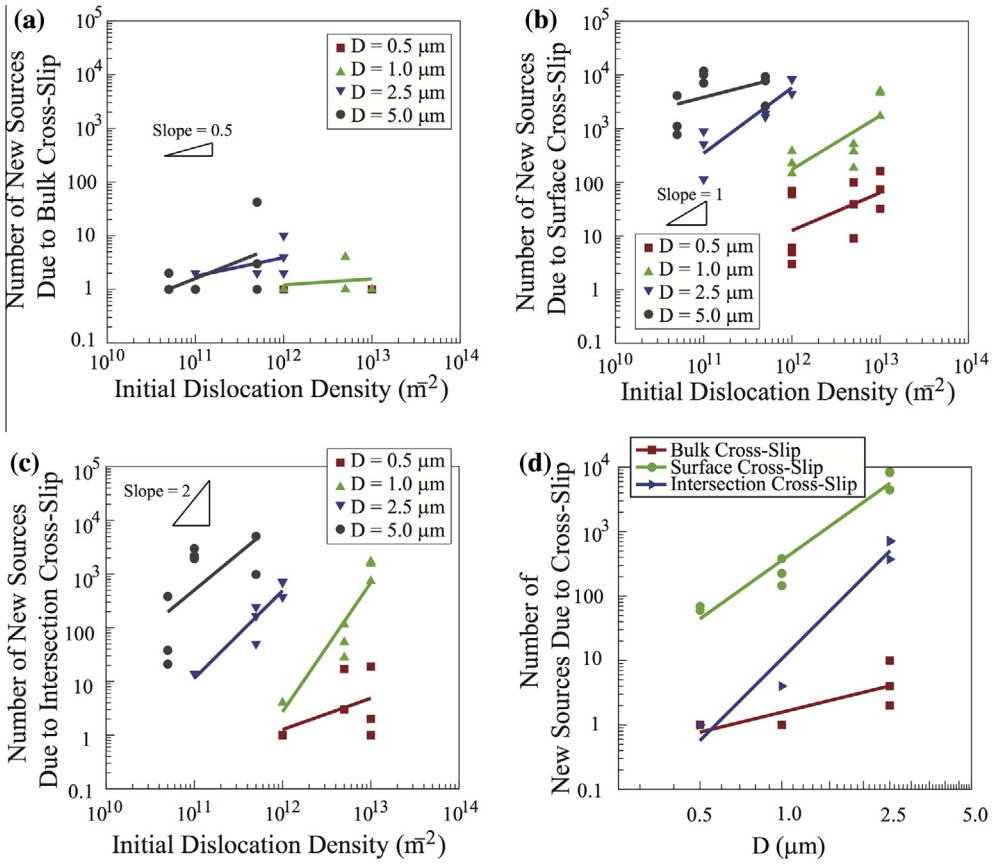

Fig. 8. Number of new dislocation sources as a function of initial dislocation density and crystal sizes due to (a) bulk cross-slip, (b) surface cross-slip, (c) intersection cross-slip and (d) number of new dislocation sources as a function of the crystal size for a given initial dislocation density of 10^{12} m^{-2} due to bulk cross-slip, surface cross-slip and intersection cross-slip.

for dislocations escaping from the free surface, which enhances the chances of intersection cross-slip.

Initially, as bulk dislocations evolve and intersect the surface, surface dislocations are created, which alters the actual number of sources of each type responsible for cross-slip. Based on the physics of each cross-slip type, as a first-order approximation it can be expected that the number of sources generated due to bulk or surface cross-slip must be proportional to the number of dislocation sources in the microcrystal. On the other hand, since the frequency of junction formation can be expected to be proportional to the square of the number of the available sources, the number of newly generated sources due to intersection cross-slip should also be expected to scale with the square of the number of dislocation sources in the microcrystal. By examining Fig. 8, and noting that the initial dislocation density is a measure of the number of sources in the system, it is observed that the slopes of the curves are roughly equal to 1.0 for surface cross-slip and 2.0 for intersection cross-slip. This is consistent with the aforementioned phenomenological discussion. However, the slope of the curves for the bulk cross-slip cases are significantly smaller ($\approx 0.1 - 0.3$), which deviates considerably from the expected linear dependence, as discussed above. This can be explained by taking into account that the activation energy of bulk cross-slip is much higher than surface or intersection cross-slip. Furthermore, given the short mean free path for bulk dislocations in microcrystals, most bulk segments, especially at low densities, will intersect the surface before they get a chance to cross-slip in the bulk, thus further reducing the rate at which bulk cross-slip generates new sources.

Finally, from the simulations performed with a single cross-slip type enabled at a time (see Fig. 5), it is possible to determine the synergistic effects of the different cross-slip types. In the simulation with only bulk cross-slip, 19 new sources were created at 0.25% strain. In the simulation with intersection cross-slip only, the number of new sources was 308 at this strain level. Finally, in the simulation with only surface cross-slip accounted for, the number of new sources was 1128. However, when all cross-slip types were accounted for, the number of events from each cross-slip type almost doubled, with 38, 708 and 1830 bulk, intersection and surface cross-slip events, respectively, recorded after 0.25% strain. This is due to the synergistic effects resulting from the activity of all cross-slip types simultaneously. For instance, as surface cross-slip is induced, the probability of junction formation increases, which subsequently increases the probability of intersection cross-slip. Furthermore, a higher density of screw dislocations are expected to traverse the crystal, which subsequently increases the probability of bulk cross-slip, and vice versa. This is consistent with the idea of source generation rate dependence on the existing number of sources. As more cross-slip types are activated, more sources are generated, which further induces source generation.

5. Summary and conclusions

In this work, three new mechanisms of cross-slip in fcc crystals that were recently identified from MD simulations were implemented into discrete dislocation dynamics simulations to study the evolution of dislocation microstructures of various crystal sizes and dislocation densities. Cross-slip event frequencies were analyzed and it was found that bulk cross-slip is the least frequent, given the calculated activation energy, and does not contribute much to the microstructure evolution. Surface cross-slip is the most frequent type, and it explains surface slip localization. Additional studies are required to adjust the pre-exponential factor in the cross-slip model in order to match the observed strain hardening rates obtained from simulations to experimentally observed ones. Overall, the observations suggest that surface and intersection cross-slip are more influential on microstructure evolution, and that emphasis should be placed on further exploration of those mechanisms.

Acknowledgements

A.M.H. and J.A.E. acknowledge the support by DARPA contract # N66001–12-1–4229, support through Grant # FA9550–12-1–0445 to the Center of Excellence on Integrated Materials Modeling (CEIMM) at Johns Hopkins University (partners JHU, UIUC, UCSB), awarded by the AFOSR/RSL and AFRL/RX, and the computing time Granted by XSEDE on their computers. S.I.R., M.D.U. and D.M.D. also acknowledge the support from AFOSR/RY (D. Stargel, program manager).

References

[1] D. Hull, D.J. Bacon, Introduction to Dislocations, Butterworth-Heinemann, 2001.
[2] P.J. Jackson, Dislocation modelling of shear in FCC crystals, Prog. Mater. Sci. 29 (1-2) (1985) 139–175.
[3] E.Y. Gutmanas, E.M. Nadgornyi, Dislocation multiplication by multiple cross slip, Sov. Phys. Solid State 12 (1970) 733–734.
[4] Y. Tang, J.A. El-Awady, Formation and slip of pyramidal dislocations in hexagonal close-packed magnesium single crystals, Acta Mater. 71 (2014) 319–332.
[5] P.J. Jackson, The role of cross-slip in the plastic deformation of crystals, Mater. Sci. Eng. 57 (1983) 39–47.
[6] G. Saada, Cross-slip and work hardening of fcc crystals, Mater. Sci. Eng. A. 137 (1991) 177–183.
[7] M.S. Duesbery, N.P. Louat, K. Sadananda, The mechanics and energetics of cross-slip, Acta Metall. Mater. 40 (1) (1992) 149–158.
[8] K. Jumonji, S. Ueta, A. Miyahara, M. Kato, A. Sato, Rapid work hardening caused by cube cross slip in Ni3Al single crystals, Philos. Mag. A 73 (1996) 345–364.
[9] J.P. Poirier, On the symmetrical role of cross-slip of screw dislocations and climb of edge dislocations as recovery process controlling high-temperature creep, Rev. Phys. Appl. 11 (1976) 731.
[10] L.P. Kubin, B. Devincre, T. Hoc, Inhibited dynamic recovery and screw dislocation annihilation in multiple slip of fcc single crystals, Philos. Mag. 86 (2006) 4023–4036.
[11] R. Madec, B. Devincre, L.P. Kubin, Simulation of dislocation patterns in multislip, Scr. Mater. 47 (10) (2002) 689–695.
[12] B. Escaig, Cross-slipping process in the fcc structure, in: Proc. Battelle Coll. Disl. Dyn., McGraw- Hill, New York, 1968, pp. 655–677.
[13] F.J. Humphreys, P.B. Hirsch, The deformation of single crystals of copper and copper-zinc alloys containing alumina particles. ii. microstructure and dislocation-particle interactions, Proc. Royal Soc. A 318 (1970) 73–92.
[14] G. Schoeck, A. Seeger, Activation energy problems associated with extended dislocations, in: Report of the Bristol Conference on Defects in Crystalline Solids, Physical Society, London, 1955, pp. 340–346.
[15] J. Friedel, Regarding seeger's paper on work hardening, in: J.C. Fisher, W.G. Johnston, R. Thromson, T. Vreeland (Eds.), Dislocations and Mechanical Properties of Crystals, John Wiley and Sons Inc., New York, 1957, pp. 330–332.
[16] R.L. Fleischer, Cross slip of extended dislocations, Acta Metall. 7 (1959) 134–135.
[17] J. Washburn, Intersection cross slip, App. Phys. Lett. 7 (1965).
[18] W. Puschl, Models for dislocation cross-slip in close-packed crystal structures: a critical review, Prog. Mat. Sci. 47 (2002) 415–461.
[19] J. Bonneville, B. Escaig, Cross-slipping process and the stress-orientation dependence in pure copper, Acta Metall. 27 (9) (1979) 1477–1486.
[20] J. Bonneville, G. Vanderschaeve, A study of cross slip in the fcc structure, in: Proc. 7th Int. Conf. Strength of Metals and Alloys, vol. 1, 1985, pp. 9–12.
[21] J. Bonneville, B. Escaig, J.L. Martin, A study of cross-slipping activation parameters in pure copper, Acta Metall. 36 (1988) 1989–2002.
[22] O. Couteau, T. Kruml, J.-L. Martin, About the activation volume for cross-slip in Cu at high stresses, Acta Mater. 59 (10) (2011) 4207–4215.
[23] T. Rasmussen, K.W. Jacobsen, T. Leffers, O.B. Pedersen, S.G. Srinivasan, H. Jónsson, Atomistic determination of cross-slip pathway and energetics, Phys. Rev. Lett. 79 (19) (1997) 3676–3679.
[24] T. Rasmussen, K.W. Jacobsen, T. Leffers, O.B. Pedersen, Simulations of the atomic structure, energetics, and cross slip of screw dislocations in copper, Phys. Rev. B 56 (1997) 2977–2990.
[25] S.I. Rao, T.A. Parthasarathy, C. Woodward, Atomistic simulation of cross-slip processes in model fcc structures, Philos. Mag. A 79 (5) (1999) 1167–1192.
[26] T. Vegge, T. Rasmussen, T. Leffers, O.B. Pedersen, K.W. Jacobsen, Atomistic simulations of cross-slip of jogged screw dislocations in copper, Philos. Mag. Lett. 81 (2001) 137–144.
[27] L.P. Kubin, G. Canova, M. Condat, B. Devincre, V. Pontikis, Y. Bréechet, Dislocation microstructures and plastic flow: a 3-D simulation, Solid State Phenom. 23–24 (1992) 455–472.
[28] H.M. Zbib, M. Rhee, J.P. Hirth, On plastic deformation and the dynamics of 3-D dislocations, J. Mech. Sci. 40 (2-3) (1998) 113–127.
[29] K.W. Schwarz, Simulation of dislocations on the mesoscopic scale, J. Appl. Phys. 85 (1) (1999) 108–129.
[30] N.M. Ghoniem, S.-H. Tong, L.Z. Sun, Parametric dislocation dynamics: a thermodynamics-based approach to investigations of mesoscopic plastic deformation, Phys. Rev. B 61 (2) (2000) 913–927.
[31] H.M. Zbib, M. Rhee, J.P. Hirth, A multiscale model of plasticity, Int. J. Plast. 18 (2002) 1133–1163.
[32] D. Weygand, L.H. Friedman, E. Van der Giessen, A. Needleman, Aspects of boundary-value problem solutions with three-dimensional dislocation dynamics, Mod. Sim. Mater. Sci. Eng. 10 (4) (2002) 437–468.
[33] A. Arsenlis, W. Cai, M. Tang, M. Rhee, T. Oppelstrup, G. Hommes, T.G. Pierce, V.V. Bulatov, Enabling strain hardening simulations with dislocation dynamics, Mod. Sim. Mater. Sci. Eng. 15 (6) (2007) 553–595.
[34] J.A. El-Awady, S.B. Biner, N.M. Ghoniem, A self-consistent boundary element, parametric dislocation dynamics formulation of plastic flow in finite volumes, J. Mech. Phys. Solids 56 (5) (2008) 2019–2035.
[35] A.A. Benzerga, Y. Brchet, A. Needleman, E. Van der Giessen, Incorporating three-dimensional mechanisms into two-

dimensional dislocation dynamics, Mod. Sim. Mater Sci. Eng. 12 (1) (2004) 159–196.
[36] A.A. Benzerga, Micro-pillar plasticity: 2.5D mesoscopic simulations, J. Mech. Phys. Solids 57 (9) (2009) 1459–1469.
[37] C. Zhou, R. Lesar, Dislocation dynamics simulations of plasticity in polycrystalline thin films, Int. J. Plast. 30-31 (2012) 185–201.
[38] P. Pant, K.W. Schwarz, S.P. Baker, Dislocation interactions in thin fcc metal films, Acta Mater. 51 (2003) 3243–3258.
[39] S.P. Baker, R.S. Fertig, Dislocation dynamics simulations of dislocation interactions and stresses in thin films, Acta Mater. 58 (2010) 5206–5218.
[40] J.A. El-Awady, M. Wen, N.M. Ghoniem, The role of the weakest-link mechanism in controlling the plasticity of micropillars, J. Mech. Phys. Solids 57 (1) (2009) 32–50.
[41] C. Motz, D. Weygand, J. Senger, P. Gumbsch, Initial dislocation structures in 3-D discrete dislocation dynamics and their influence on microscale plasticity, Acta Mater. 57 (6) (2009) 1744–1754.
[42] C. Zhou, I.J. Beyerlein, R. LeSar, Plastic deformation mechanisms of fcc single crystals at small scales, Acta Mater. 59 (20) (2011) 7673–7682.
[43] J.A. El-Awady, M.D. Uchic, P. Shade, S.-L. Kim, S.I. Rao, D.M. Dimiduk, C. Woodward, Pre-straining effects on the power-law scaling of size-dependent strengthening in ni single crystals, Scr. Mater. 68 (2013) 207–210.
[44] T.A. Khraishi, H.M. Zbib, T. Diaz de la Rubia, M. Victoria, Modelling of irradiation-induced hardening in metals using dislocation dynamics, Philos. Mag. Lett. 81 (2001) 583–593.
[45] M.C. Fivel, C.F. Robertson, G.R. Canova, L. Boulanger, Three-dimensional modeling of indent-induced plastic zone at a mesoscale, Acta Mater. 46 (1998) 6183–6194.
[46] Y. Gao, Z. Zhuang, Z.L. Liu, X.C. You, X.C. Zhao, Z.H. Zhang, Investigations of pipe-diffusion-based dislocation climb by discrete dislocation dynamics, Int. J. Plast. 27 (2011) 1055–1071.
[47] Z.Q. Wang, I.J. Beyerlein, R. LeSar, Plastic anisotropy in fcc single crystals in high rate deformation, Int. J. Plast. 25 (1) (2009) 26–48.
[48] M. Verdier, M. Fivel, I. Groma, Mesoscopic scale simulation of dislocation dynamics in fcc metals: principles and applications, Mod. Sim. Mater. Sci. Eng. 6 (6) (1998) 755–770.
[49] C. Depres, C.F. Robertson, M.C. Fivel, Low strain fatigue in 316L steel surface grains: a three-dimension discrete dislocation dynamics modeling of the early cycles. part 2: persistent slip markings and micro-crack nucleation, Philos. Mag. 86 (1) (2006) 79–97.
[50] K. Kang, J. Yin, W. Cai, Stress dependence of cross slip energy barrier for face-centered cubic nickel, J. Mech. Phys. Solids 62 (0) (2014) 181–193.
[51] S.I. Rao, D.M. Dimiduk, J.A. El-Awady, T.A. Parthasarathy, M.D. Uchic, C. Woodward, Atomistic simulations of athermal cross-slip nucleation at screw dislocation intersections in face-centered cubic nickel, Philos. Mag. 89 (34–36) (2009) 3351–3369.
[52] S.I. Rao, D.M. Dimiduk, J.A. El-Awady, T.A. Parthasarathy, M.D. Uchic, C. Woodward, Activated states for cross-slip at screw dislocation intersections in face-centered cubic nickel and copper via atomistic simulation, Acta Mater. 58 (2010) 5547–5557.
[53] S.I. Rao, D.M. Dimiduk, T.A. Parthasarathy, J. El-Awady, C. Woodward, M.D. Uchic, Calculations of intersection cross-slip activation energies in fcc metals using nudged elastic band method, Acta Mater. 59 (19) (2011) 7135–7144.
[54] S.I. Rao, D.M. Dimiduk, J.A. El-Awady, T.A. Parthasarathy, M.D. Uchic, C. Woodward, Spontaneous athermal cross-slip nucleation at screw dislocation intersections in fcc metals and L12 intermetallics investigated via atomistic simulations, Philos. Mag. 93 (22) (2013) 3012–3028.
[55] S.I. Rao, D.M. Dimiduk, T.A. Parthasarathy, M.D. Uchic, C. Woodward, Atomistic simulations of surface cross-slip nucleation in face-centered cubic nickel and copper, Acta Mater. 61 (7) (2013) 2500–2508.
[56] B. Jakobsen, U. Lienert, J. Almer, W. Pantleon, H. F Poulsen, Properties and dynamics of bulk subgrains probed in-situ using a novel x-ray diffraction method, Mater. Sci. Forum 550 (2007) 613–618.
[57] D.M. Norfleet, D.M. Dimiduk, S.J. Polasik, M.D. Uchic, M.J. Mills, Dislocation structures and their relationship to strength in deformed nickel microcrystals, Acta Mater. 56 (13) (2008) 2008.
[58] G Makov P Landau, R Z Shneck, A. Venkert, Evolution of dislocation patterns in fcc metals, IOP Conf. Ser. Mater. Sci. Eng. 3 (2009).
[59] D.M. Dimiduk, M.D. Uchic, T.A. Parthasarathy, Size-affected single-slip behavior of pure nickel microcrystals, Acta Mater. 53 (15) (2005) 4065–4077.
[60] E. Göttler, Dislocation structure and work-hardening of copper single crystals with [100] axis orientation: I. dislocation arrangement and cell structure of crystals deformed in tension, Philos. Mag. 28 (1973) 1057–1976.
[61] P. Landau, R.Z. Shneck, G. Makov, A. Venkert, In-situ tem study of dislocation patterning during deformation in single crystal aluminum, J. Phys. 241 (1) (2010) 012060.
[62] Q. Yu, R.K. Mishra, J.W. Morris, A.M. Minor, The effect of size on dislocation cell formation and strain hardening in aluminum, Philos. Mag. 94 (2014) 2062–2071.
[63] J.A. El-Awady, Unraveling the physics of size dependent dislocation mediated plasticity, Nature Commun. (2014), accepted for publication.
[64] S.I. Rao, D.M. Dimiduk, T.A. Parthasarathy, M.D. Uchic, M. Tang, C. Woodward, Athermal mechanisms of size-dependent crystal flow gleaned from three-dimensional discrete dislocation simulations, Acta Mater. 56 (13) (2008) 3245–3259.
[65] B. Devincre, L.P. Kubin, Mesoscopic simulations of dislocations and plasticity, Mater. Sci. Eng. A 234-236 (1997) 8–14.
[66] H. Neuhauser, Slip propagation and fine structure, Solid State Phen. 3–4 (1991) 407–415.
[67] Y.W. Zhang, T.C. Wang, N.G. Liang, The inhomogeneity of plastic deformation in ductile single crystals, Mod. Sim. Mater. Sci. Eng. 2 (6) (1994) 1171.
[68] M.D. Uchic, P.A. Shade, D.M. Dimiduk, Plasticity of micrometer-scale single crystals in compression: a critical review, Annu. Rev. Mater. Res. 39 (1) (2009) 361–386.
[69] J.R. Greer, J.Th.M. De Hosson, Plasticity in small-sized metallic systems: Intrinsic versus extrinsic size effect, Prog. Mater. Sci. 56 (6) (2011) 654–724.
[70] A. El-Azab, Statistical mechanics of dislocation systems, Scr. Mater. 54 (5) (2006) 723–727.